Soils and Rocks
An International Journal of Geotechnical and Geoenvironmental Engineering
www.soilsandrocks.com
ISSN 1980-9743
ISSN-e 2675-5475

# Comparison between machine learning techniques to predict sand/geomembrane interface shear strength

Anderson Villamil[1], Abenezer Tefera Tanga[1], Gregório Luís Silva Araújo[1#], Francisco Evangelista Junior[1]

Article

**Keywords**
Artificial intelligence
Geosynthetics
Interfaces
Machine Learning
Pearson's correlation
Shear strength

**Abstract**

Geomembranes (GM) have been extensively used for waterproofing applications, and often they are in contact with soil materials or other geosynthetics for mechanical protection. Strength evaluation at the interface between the GM and the contact material is fundamental to ensure a good design that guarantees a low probability of this interface failure. This paper analyses and compares four Artificial Neural Network (ANN) models (varying the number of inputs and hidden layers) and the Random Forest (RF) technique to predict sand/GM interface shear strength based on 495 results from previous investigations. All models were optimized with the Differential Evolution (DE) algorithm. The Coefficient of Determination ($R^2$) and root mean squared error (*RMSE*) were set as evaluation criteria for the accuracy of the developed models. The results show that RF performs best as a prediction tool for the data analysed. Data correlation and RF feature importance analysis were also conducted, establishing GM asperity height as the most significant variable for the collected data. The results show the great potential of Machine Learning applications for predicting the interface shear strength between sand and geomembranes in geotechnical engineering constructions.

## 1. Introduction

Geosynthetics have emerged as a widely used solution for solving geotechnical challenges in civil engineering projects. Geomembranes (GM) are mainly used as a waterproofing system due to their low permeability and good mechanical behaviour (Koerner, 2012), establishing effective control and management of liquids, minimizing the possibility of infiltration. In this context, it is crucial to establish a sufficient interface shear strength between the geosynthetic and the surrounding soil to ensure the strength and integrity of these structures and prevent potential failures (Moraci et al., 2014). This interface shear strength is often quantified by determining the friction angle, which can be evaluated through various laboratory tests such as direct shear, ring shear, pull-out, or inclined plane tests (Palmeira, 2009; Moraci et al., 2014; Cen et al., 2018).

Various researchers performed multiple investigations using a variety of soil and geomembranes to assess the interface resistance. The results have shown that relevant several influential factors affect the strength parameters in addition to the type of test employed. These factors include geomembrane characteristics, such as type, thickness and asperity height, or soil type, and external conditions like applied normal stresses and contact area (Izgin, 1997; Wasti & Özdüzgün, 2001; Palmeira et al., 2002; Rebelo, 2003; Aguiar, 2008; Pitanga et al., 2009; Moraci et al., 2014; Alzahrani, 2017; Sánchez, 2018; Lashkari & Jamali, 2021; Araújo et al., 2022; Khan & Latha, 2023; Costa Junior et al., 2023).

Machine learning (ML), which is related to Artificial Intelligence (AI), is a computational technique capable of evaluating and learning from prior information (data mining) to forecast or categorize a response, employing algorithms and statistical calculations without complicated programming. AI has gained attention in civil engineering due to its versatility, simplicity of application, and ability to solve complex problems (Lu et al., 2012; Shahin, 2013; Evangelista Junior & Afanador-García, 2016; Dede et al., 2019; Huang et al., 2019; Evangelista Junior & Almeida, 2021; Lagaros & Plevris, 2022; Xu et al., 2023; Silva et al., 2023, Lima et al., 2023a) and has great potential to predict the interface shear strength between geosynthtetics and other materials.

[#]Corresponding author. E-mail address: gregorio@unb.br
[1]Universidade de Brasília, Departamento de Engenharia Civil e Ambiental, Brasilia, DF, Brasil.

Submitted on March 12, 2025; Final Acceptance on September 5, 2025; Discussion open until May 31, 2026.
Editor: Renato P. Cunha
https://doi.org/10.28927/SR.2026.004425

Several papers can be found in the last recent years regarding Artificial Intelligence and geosynthetics, (Kumari & Dutta, 2019; Raja & Shukla, 2021; Pant & Ramana, 2022; Ali et al., 2022; Raja et al., 2022; Tan et al., 2022; Hasthi et al., 2022; Li et al., 2025). However, although previous studies for soil-geosynthetic interface behaviour assessment with ML techniques, many of them have less than 400 laboratory results and just used one type of test (Debnath & Dey, 2017; Chao et al., 2021, 2023; Ali et al., 2022; Pant & Ramana, 2022). In this manner, it is important to evaluate how a dataset from different types of experiments can improve the prediction of the interface shear strength between geomembrane and other materials such as sand.

This paper evaluates and compares the results of two ML methodologies: (i) four different Artificial Neural Network (ANN) architectures and (ii) non-linear Random Forest (RF) approach to predict the interface friction angle between sand and geomembrane. The Differential Evolution optimization algorithm was conducted in both methods. The analysis was carried out using an input parameters data collection comprised of 495 samples obtained from three different laboratory tests conducted in previous studies (manufacturer company, scientific papers, Master dissertations and PhD-thesis) produced in seven countries. The idea of using different type of tests is trying to improve the ML learning process. Two statistical metrics, the $R^2$ and *RMSE*, were used to establish the best accurate prediction model between ANN and RF. Additionally, Pearson's linear correlation and non-linear RF feature importance were conducted evaluating the main impact factors in soil-GM shear strength interface for the collected data.

## 2. Machine learning algorithms used

In the literature, there are studies developed for predicting soil-geosynthetic interface resistance using ANN (Debnath & Dey, 2017; Chao et al., 2021, 2023; Ali et al., 2022) and RF (Pant & Ramana, 2022). However, these only focused on the use of one type of test with limited data and did not compare the techniques herein applied. In this study the evaluation and comparison between the two methodologies is apply to define the best prediction algorithm.

### 2.1 Artificial Neural Network (ANN)

An ANN corresponds to a computational model developed by algorithms which mimic biological neuronal characteristics (Fausett, 1994; Basheer & Hajmeer, 2000; Shahin et al., 2009). Multi-Layer Perceptron (MLP) is one of the most widely used architectures in ANNs, where neurons are organized into input, hidden layers, and output (Shahin et al., 2008). Figure 1 shows a general architecture for an MLP network.

Another significant feature of ANN is the learning rule that establishes the training process. The Backpropagation (BP) training algorithm is one of the most widely method applied (Soleimanbeigi & Hataf, 2006) and has been used in this investigation.

### 2.2 Random Forest (RF)

RF is a supervised ML algorithm developed by Breiman (2001) that combines the Decision Trees methodology with regression and is trained using the bootstrap aggregating (bagging) method (Géron, 2019). According to Pant & Ramana (2022), RF is built upon the concept of bagging decision trees, where multiple subsamples are generated from the original dataset.

As shown in Figure 2, the training input is divided using the k-fold cross-validation technique in each subsample. One part of the division derives the regression function from a new training dataset for each decision tree. The other omitted part, known as out-of-bag (OOB), is used to evaluate the accuracy of each subsample.

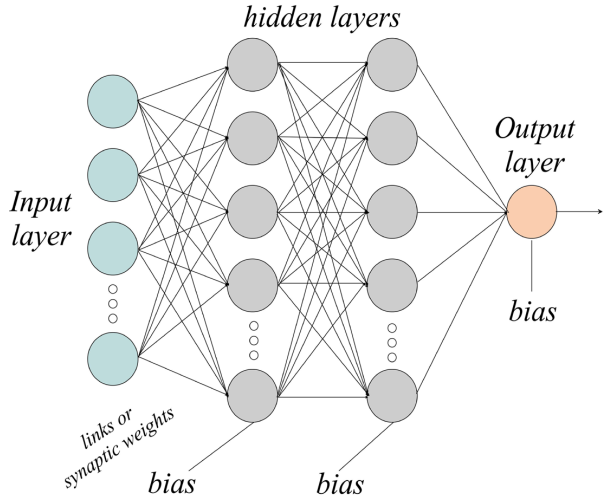


**Figure 1.** Multilayer Perceptron Network general architecture.

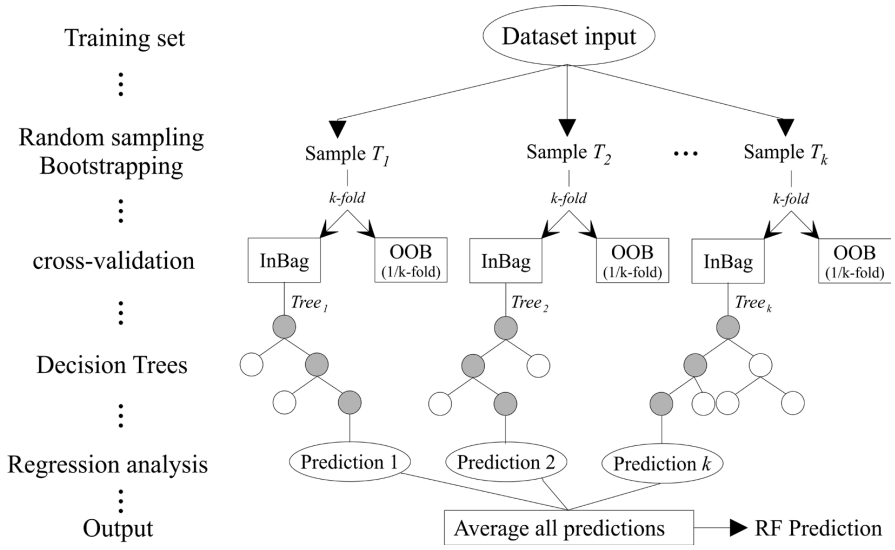


**Figure 2.** RF model architecture.

### 2.3 Hyperparameter optimisation (HPO) – Differential Evolution (DE)

In machine learning, certain parameters are used during training control as a portion of the learning, analysis, and outcome prediction. However, some parameters are set beforehand and remain constant during model training. These parameters are known as hyperparameters, which can be optimized to significantly improve the performance of the chosen model algorithm (Hutter et al., 2019; Lima et al., 2023b). The optimization algorithm aims to identify the optimal hyperparameters values (best combination) for prediction analysis.

Differential Evolution (DE) is a heuristic optimization algorithm based on the theory of species evolution known as Evolutionary Algorithms (EA). First introduced by Storn & Price (1996), DE optimizes nonlinear and non-differentiable functions and a full description of the DE workflow is presented in Atangana Njock et al. (2023). Figure 3 shows the optimization process in both ML-implemented techniques used in this study.

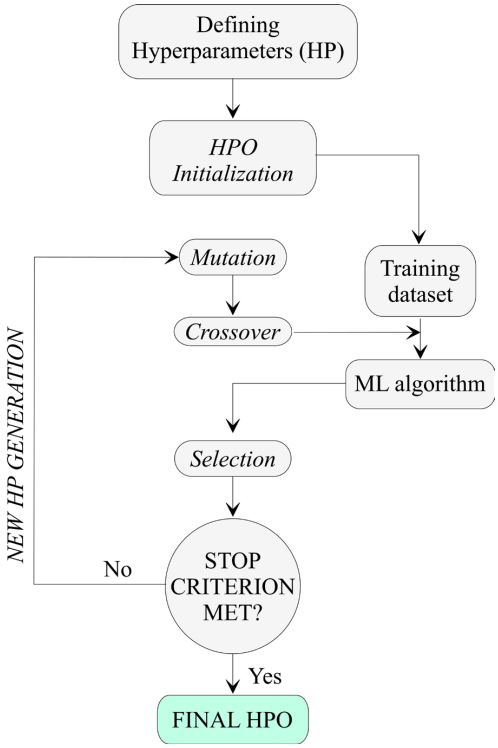


**Figure 3.** Flowchart of DE-ML algorithm implementation.

## 3. Data mining and correlation

Considering that the selected ML methodologies correspond to a supervised learning type, it is necessary to have input data and known result values. Based on this, a search was conducted for laboratory test results evaluating the interface strength between sand and geomembrane. Four hundred sixty samples were collected from previous research available in the literature, and an additional 35 samples were provided by a geomembrane manufacturer. The reference data were chosen considering the most common detailed information in each study regarding twelve influencing parameters as input: (1) applied normal stress, (2) coefficient of curvature, (3) contact area, (4) displacement rate, (5) GM asperity height, (6) GM thickness, (7) median grain size, (8) sand density index, (9) soil friction angle, (10) soil unit mass, (11) type of implemented test (Conventional Direct Shear – *CDS*, Medium Direct Shear – *MDS*, or Inclined Plane – *IP*), and (12) uniformity coefficient. Figure 4 shows the location of the selected studies and their respective reference.

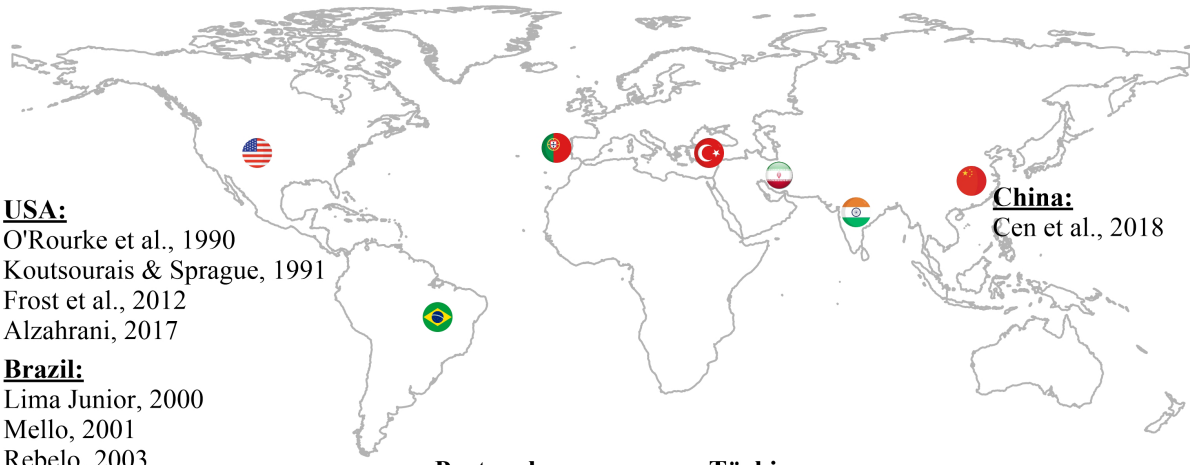


**Figure 4.** Dataset reference location. Source: O'Rourke et al. (1990), Koutsourais & Sprague (1991), Frost et al. (2012), Alzahrani (2017), Lima Junior (2000), Mello (2001), Rebelo (2003), Palmeira et al. (2002), Viana (2007), Sánchez (2018), Industry Data (2021), Lopes et al. (2001), Izgin (1997), Vangla & Gali (2016), Lashkari & Jamali (2021) and Cen et al. (2018).

**Table 1.** Statistical information of influence parameters.

| | Parameter | Min | Max | Mean | $\sigma_{STD}$ | $CV$ |
|---|---|---|---|---|---|---|
| | Input | | | | | |
| $R_d$ | Displacement rate (mm/min) | 0.10 | 3.00 | 1.11 | 0.67 | 0.60 |
| $\sigma_n$ | Normal stress (kPa) | 1.00 | 300.00 | 43.59 | 48.77 | 1.12 |
| $A_c$ | Contact area (cm$^2$) | 36.00 | 9024.00 | 1521.00 | 2994.94 | 1.97 |
| $t$ | GM thickness (mm) | 0.50 | 3.00 | 1.68 | 0.45 | 0.27 |
| $A_h$ | GM asperity h (mm) | 0.00 | 1.71 | 0.18 | 0.45 | 2.48 |
| $I_d$ | Sand relative density (%) | 20.80 | 98.00 | 57.83 | 24.43 | 0.42 |
| $\gamma$ | Soil unit weight (kN/m$^3$) | 14.5 | 29.4 | 15.5 | 2.9 | 1.8 |
| $C_c$ | Coefficient of curvature | 0.80 | 1.68 | 1.03 | 0.37 | 0.36 |
| $C_u$ | Uniformity coefficient | 1.11 | 46.80 | 2.82 | 5.92 | 2.09 |
| $D_{50}$ | Median grain size (mm) | 0.17 | 3.08 | 0.58 | 0.60 | 1.04 |
| $\phi_s$ | Friction angle of soil (°) | 25.30 | 49.50 | 38.30 | 4.99 | 0.13 |
| | Type of test | *CDS*: 121; *MDS*: 122; *IP*: 252 | | | | |
| | Output | | | | | |
| $\delta'$ | Friction angle interface (°) | 7.50 | 64.50 | 28.20 | 7.32 | 0.26 |

Legend: see List of symbols and abbreviations.

Table 1 shows the statistical data of the influencing parameters used. The statistical information of the collected data reveals a wide distribution for each parameter, enabling a better characterization and analysis for different soil and geomembrane conditions. This is reflected in the high coefficient of variation (*CV*) values for some parameters, such as normal stress and contact area (significant variability due to the type and conditions of test execution), asperity height (from smooth to rough GM with maximum values of 1.71 mm), and uniformity coefficient (associated with a wide range of variety in the type of used sand). It is essential to point out that the "Test Type" parameter was defined with values of 0 or 1. A value of 1 was assigned when *CDS*, *MDS* or *IP* tests were conducted.

### 3.1 Linear data correlation

The Pearson correlation coefficient ($\rho_r$) is a statistical measure used to quantify the strength and direction of the linear relationship between two variables. It is calculated based on the covariance of the variables, normalized by the product of their standard deviations. The coefficient can assume values ranging from −1 to +1. A value close to zero indicates little or no linear correlation, while values closer to the extremes represent stronger correlations. A positive coefficient signifies that both variables tend to increase or decrease together (direct relationship), whereas a negative coefficient indicates that one variable tends to increase as the other decreases (inverse relationship) (Schober et al., 2018). The correlation between the influencing factors and the interface shear strength obtained from laboratory tests is shown in Figure 5, with each independent parameter's specific relationship expressed in the bottom row.

According to the correlation analysis, the asperity height of the geomembrane ($A_h$) has the strongest correlation with the interface strength ($\rho_r$= 0.64). This behaviour is aligned with the results of various studies where an increase in geomembrane roughness leads to an increase in interface strength (Stark et al., 1996; Lopes et al., 2001; Frost et al., 2012; Araújo et al., 2022; Costa Junior et al., 2023).

The sand properties also show significantly correlation to the interface strength, but with less proportion. On the other hand, the mean particle diameter $D_{50}$ ($\rho_r$= -0.24) and the coefficient of curvature $C_c$ ($\rho_r$= -0.11) show an inversely proportional relation to interface shear strength, differing from some research outcomes where it was observed a direct influence of soil properties according just to the laboratory test results (Izgin & Wasti, 1998; Lopes et al., 2001; Costa e Lopes, 2001; Afonso, 2009; Choudhary & Krishna, 2016; Markou & Evangelou, 2018; Cen et al., 2018). Conversely, the contact area exhibits a weaker correlation value ($\rho_r$ = -0.07), which is opposing to some authors' conclusions who found out that the interface friction angle presented variable behaviour across different box sizes, indicating that the contact area plays a significant role in determining the friction angle (Izgin & Wasti, 1998; Wasti & Özdüzgün, 2001; Hsieh & Hsieh, 2003; Reyes Ramirez & Gourc, 2003; Gourc & Reyes Ramírez, 2004; Aguiar, 2008; Pitanga et al., 2009; Moraci et al., 2014). The observed differences between the experimental investigations and the linear correlation can be attributed to the fact that the linear correlation calculations do not consider the influence of other variables affecting the interface friction angle.

There is an even weaker correlation observed between geomembrane thickness ($\rho_r$= -0.04) and interface friction angle. This finding is consistent with the studies conducted by Lima Junior (2000) and Sánchez (2018), who also reported a lack of direct influence between geosynthetic thickness and interface shear strength in their laboratory investigations.

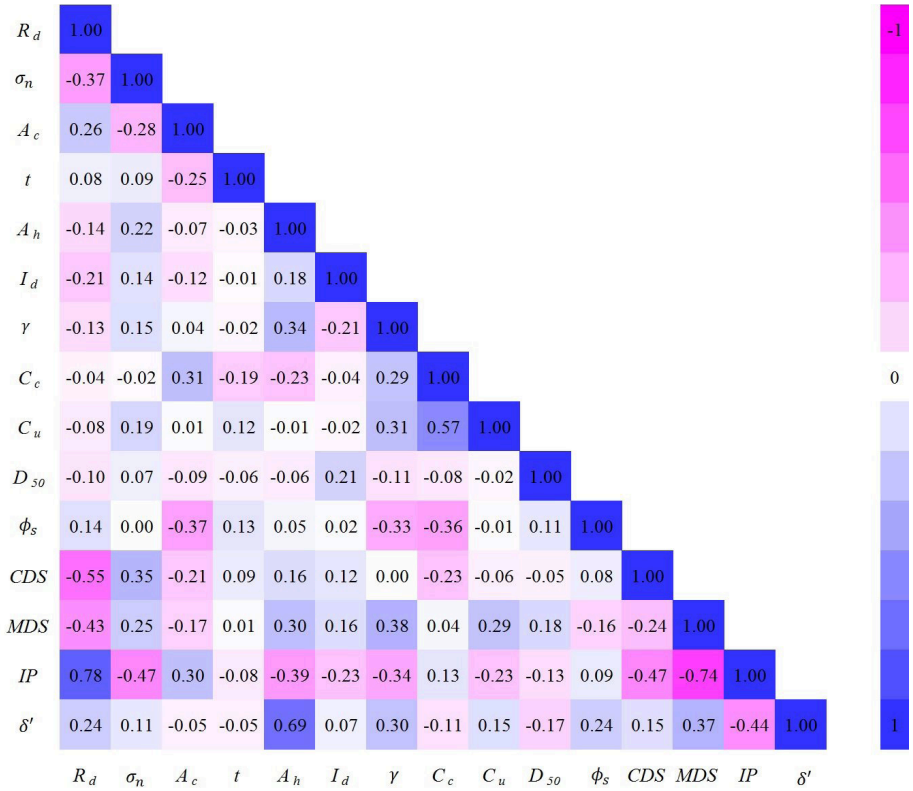


**Figure 5.** Pearson correlation heatmap between parameters and interface laboratory results.

Based on the correlation values, it can be inferred that the *MDS* test has a more significant and direct impact on determining the interface friction angle, likely linked to higher shear strength results (Hsieh et al., 2002). Conversely, the *IP* test, despite its high correlation value, outlined a negative sign which suggests that lower values of the interface friction angle may be obtained when this test is conducted. Moraci et al. (2014) and Pavanello et al. (2021) mentioned that the interface strength values for low stresses obtained in *IP* tests are lower than those obtained in direct shear tests.

## 4. Model development and implementation

### 4.1 ANN architecture

Before initiating the neural network training process, it is crucial to establish its architecture. In this research, four distinct ANN models were developed for comparison, with variations in the number of neurons in the input layer. Specifically, two models had 14 neurons in the input layer, representing all influential parameters. The other two models excluded the nominal parameter (test type) and the two parameters with the weakest correlation, namely contact area ($A_c$) and GM thickness ($t$), resulting in nine neurons in the input layer. The models differed in the number of hidden layers, ranging from one to two. The output layer consisted of a single neuron representing the interface shear strength.

The selection of the HPO corresponds to the number of hidden neurons, activation function type (logistic sigmoid, hyperbolic tangent, or ReLU function), learning rate, and momentum coefficient (Yu & Zhu, 2020; Silva et al., 2023). The activation function is fundamental in defining a neuron's output, as it transforms the aggregated weighted inputs into a specific level that governs the neuron activation. The learning rate controls the step size during weight updates, where excessively high values may induce oscillatory behaviour and harder convergence, while excessively low values demand an increased number of iterations. The momentum coefficient incorporates prior weight increments from previous iterations to improve learning and avoid local minima, however, excessive momentum may lead to overshoot minima, whereas low values yield slow convergence. Optimal tuning of those aforementioned hyperparameters is therefore critical to ensure stable, efficient, and accelerated neural network training (Diaz et al., 2017; Lima et al., 2023b).

The hyperparameters were defined based on the lowest coefficient of determination ($R^2$), obtained using the optimization algorithm (DE) in combination with the Back-Propagation algorithm. All models used the ReLU activation function, which was the most efficient among the three activation functions studied (Glorot et al., 2011). Table 2 details the value of HPO for each defined model. The four selected models correspond to the networks with the best analysis results obtained for one and two hidden layers. It is noticed that the higher the number of hidden layers, the best the predictions. However, previous analysis showed that the improvement of the predicted values for larger amounts of hidden layers did not increase much compared to the quantities herein used. Therefore, these numbers were selected once they demanded shorter processing time.

### 4.2 RF approach

Non-linear analysis approaches were evaluated using the RF methodology, examining the influence of parameter correlation methods on the prediction analysis. The RF model was optimized using the DE algorithm, where the following hyperparameters and its amount optimized were established: the number of decision trees (103), the maximum depth of each tree (30), and the minimum number of samples per split node (4).

### 4.3 Training and testing process

In various ML techniques, the learning of the model is developed in the training phase. Using the total data in this stage could lead to generalisation errors; therefore, a testing phase is included to check the model performance. The data must be split into training and testing sets to perform the analysis. A commonly used training/test ratio is 70/30% or 80/20% respectively (Jeremiah et al., 2021). In this study, both ANN and RF models adopted a random distribution data of 80% for training and 20% for testing.

### 4.4 Software implementation

The ANN and RF models described previously were implemented and executed using the Machine Learning module of the Tyche software (Tyche, 2023) developed at the Computational Methods and Artificial Intelligence Laboratory (LAMCIA) of the University of Brasilia; the software also includes hyperparameter optimization (HPO) strategies.

**Table 2.** ANN HPO values.

| Model | No. Inputs | No. Hidden layers | No. Hidden neurons | Learning rate | Momentum coefficient |
|---|---|---|---|---|---|
| 1 | 9 | 1 | 60 | 9.25 | 0.70 |
| 2 | 9 | 2 | 44/42 | 61.89 | 0.50 |
| 3 | 14 | 1 | 30 | 0.003 | 0.98 |
| 4 | 14 | 2 | 71/342 | 2.33 | 0.30 |

The codes have been successfully utilized by other studies (Oliveira et al., 2019; Borges et al., 2020; Evangelista Junior & Almeida, 2021; Chaves et al., 2023; Lima et al., 2023a, b; Silva et al., 2023).

### 4.5 Performance metrics criteria

The performance of the ANN and RF models was validated using statistical analysis by comparing the predicted values with the actual results in the dataset of the Sand-GM shear strength interface. This procedure is carried out for both the training and testing phase. The Coefficient of Determination ($R^2$) and the Root Mean Squared Error (*RMSE*) were used as evaluation methods for the models, which are given in Equation 1 and Equation 2, respectively. Error-values close to 0 and $R^2$ close to 1 outline a better model performance.

$$R^2 = 1 - \frac{\sum_{i=1}^{n}\left(y_i - \hat{y}_i\right)^2}{\sum_{i=1}^{n}\left(y_i - \overline{y}\right)^2} \quad (1)$$

$$RMSE = \sqrt{\frac{1}{n} * \sum_{i=1}^{n}\left(y_i - \hat{y}_i\right)^2} \quad (2)$$

where $n$ is the number of data, $y_i$ is the observed value, $\hat{y}_i$ the predicted value and $\overline{y}$ the mean of the observed values.

## 5. Results and discussions

### 5.1 Model performance assessment

Once the predicted values are computed in each model and phase (training and testing), they can be compared to the actual values obtained from the laboratory tests gathered in the reference data. These comparisons are presented graphically in Figure 6 and Figure 7 and are also summarized in Table 3. The regression line in the centre of the graphs represents the relationship between the two data sets. The proximity of the data points to the trend line indicates a high $R^2$ value, which is a better accuracy of the model predictions. For ANN model (Figure 6a-d and Figure 7a-d), the sequence of the numbers is: number of input parameters, number of neurons in each hidden layer (according to Table 2, models 1 and 3 have one hidden layers and model 2 and 4 with two hidden layers), and the amount of output parameter.

As observed in the results, for this study, using a higher number of inputs leads to greater accuracy (higher $R^2$ and lower *RMSE*) in the predicted data according to the compared statistical criteria for the ANN models. Incorporating GM thickness, type of test, and contact area into the analysis enhances the model's learning process, even though these parameters may exhibit low linear correlation or correspond to nominal values. The two-layer model shows a better learning process, as the $R^2$ value is higher than the one-layer model. A similar condition was observed by Ali et al. (2022), who evaluated and compared three ANN models varying the number of neurons, algorithms, and hidden layers for predicting the pull-out capacity of geosynthetic reinforced soil. It is also possible to observe that the RF methodology indicated a better performance between the input parameters and the interface interaction compared to the ANN models.

According to the results, the ANN model with 14 inputs with two hidden layers and the nonlinear model of the RF methodology demonstrate the highest accuracy in predicting the sand-GM interface shear strength values. From a statistical perspective, both models outlined reasonable predictions. However, the random forest model obtained the higher $R^2$ value and lower *RMSE* in training and testing sets.

The percentages of residual values exceeding ± 5°, which represents the difference between the predicted and actual friction angles, were calculated for each phase to also validate the model accuracy. The ANN model shows 4% and 11.6% for the training and testing data set, respectively, while the RF model showed 3% and 8.1% for the training and testing data set, respectively. This relation indicates that for the used data, the later methodology (RF) is more accurate. Figure 8 and Figure 9 displays the frequency histograms of the aforementioned residual values. The disparities between predicted and actual values may stem from the statistical variability in the collected data for the various parameters utilized. This variability enhances the training process of the network (or other ML techniques). However, the model incorporates correlation factors between each data point to establish a response, which can result in outcome variations.

**Table 3.** Performance results of all ML models.

| ML Algorithm | Model | Description | Training | | Testing | |
|---|---|---|---|---|---|---|
| | | | $R^2$ | *RMSE* | $R^2$ | *RMSE* |
| ANN | 1 | 1 h-layer, 9 inputs | 0.871 | 2.49 | 0.734 | 3.50 |
| | 2 | 2 h-layer, 9 inputs | 0.888 | 2.32 | 0.721 | 3.61 |
| | 3 | 1 h-layer, 14 inputs | 0.916 | 2.00 | 0.780 | 3.22 |
| | 4 | 2 h-layer, 14 inputs | 0.919 | 1.92 | 0.852 | 3.36 |
| Linear analysis | 1 | Linear approach | 0.630 | 4.25 | 0.630 | 5.07 |
| RF | 1 | Non-linear approach | 0.930 | 1.94 | 0.920 | 2.09 |

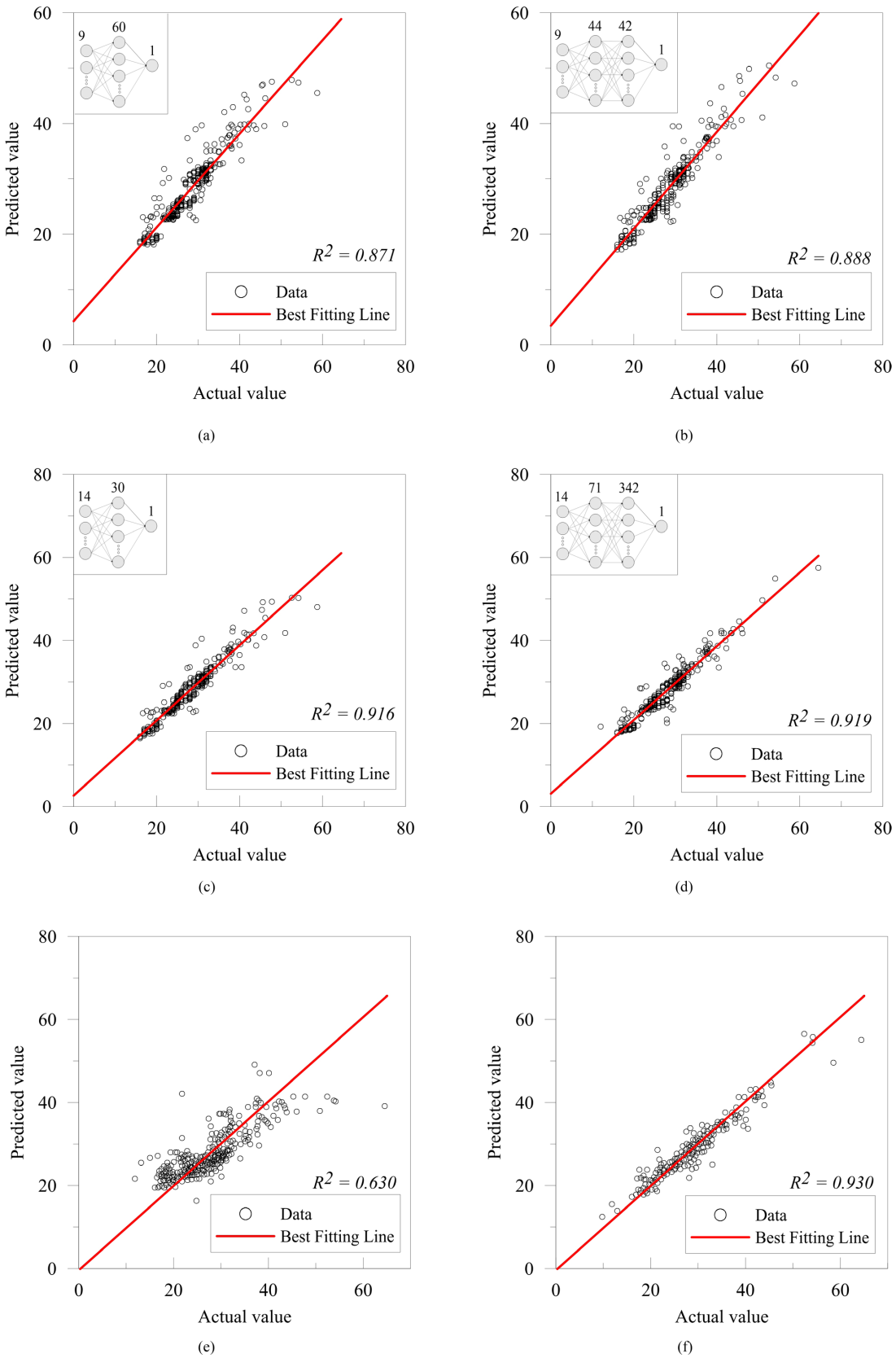


**Figure 6.** Actual and predicted interface friction angle between geomembrane and sand values for training dataset in each model: (a) Model ANN 9-60-1; (b) Model ANN 9-44-42-1; (c) Model ANN 14-30-1; (d) Model ANN 14-71-342-1; (e) linear analysis and (f) Model RF non-linear.

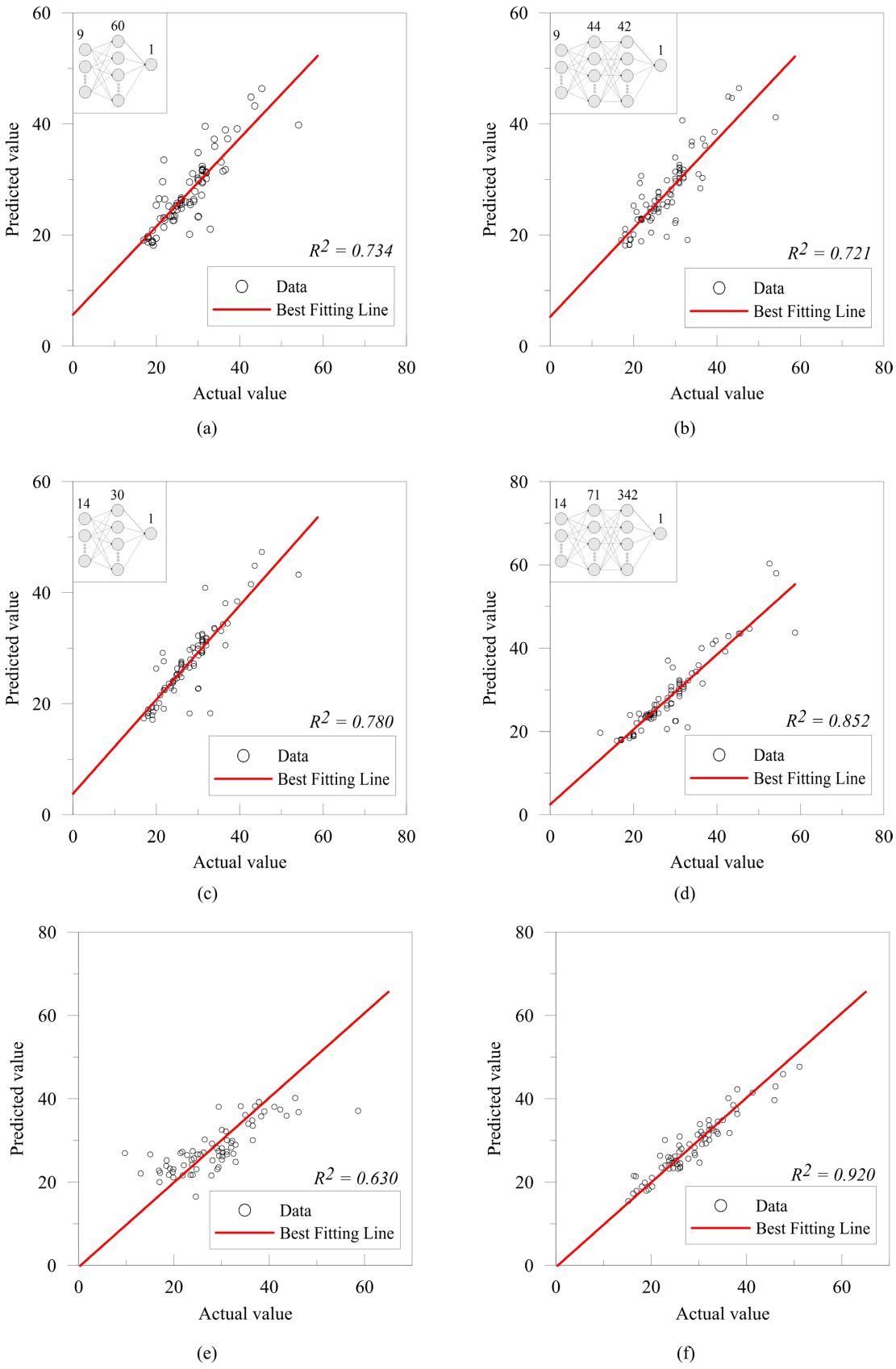


**Figure 7.** Actual and predicted values for testing dataset in each model: (a) Model ANN 9-60-1; (b) Model ANN 9-44-42-1; (c) Model ANN 14-30-1; (d) Model ANN 14-71-342-1; (e) linear analysis and (f) Model RF non-linear.

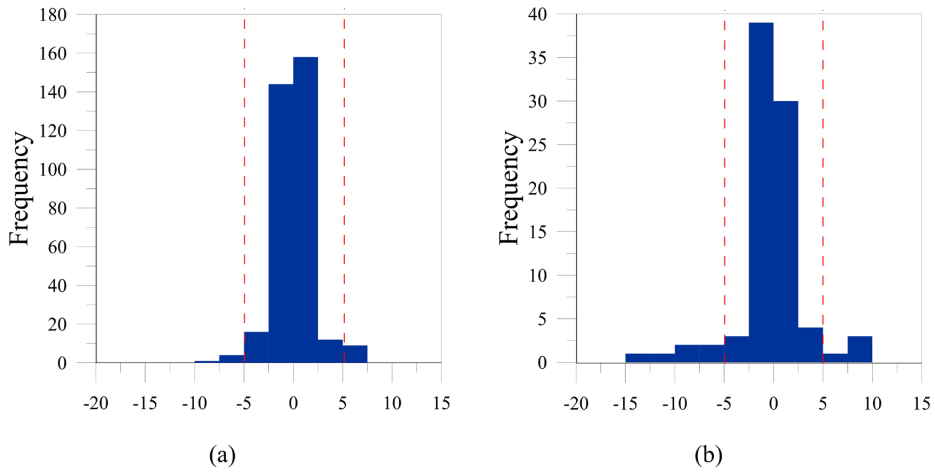


**Figure 8.** Histogram of residual values for ANN model: (a) Training set; (b) Testing set.

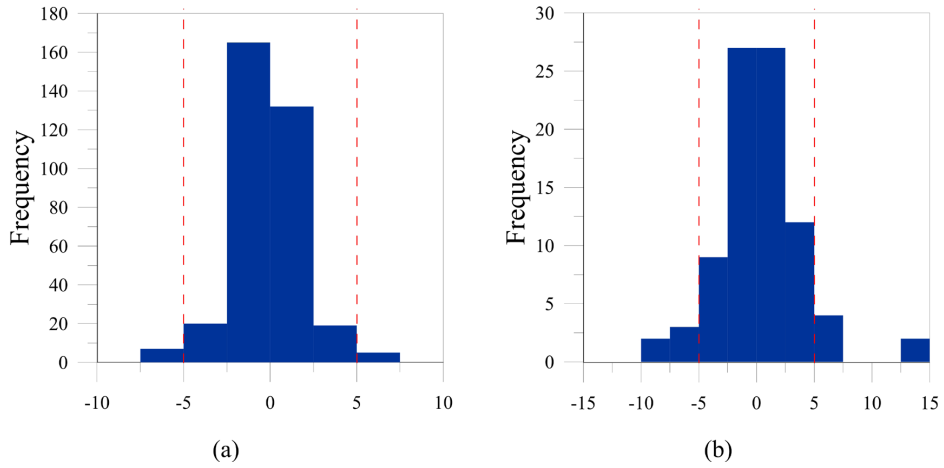


**Figure 9.** Histogram of residual values for RF model: (a) Training set; (b) Testing set.

A greater quantity of samples could enhance the network's training phase, potentially leading to increased accuracy in residual values (Chao et al., 2021; Hasthi et al., 2022).

### 5.2 Feature importance analysis

The random forest algorithm can evaluate the significance of a variable by examining the impact on prediction error. In contrast, the OOB data for that variable is randomly permuted and keeps other variables unchanged (Liaw & Wiener, 2002) and the variable values are shuffled randomly for the OOB observations to determine the importance of a specific predictor. The difference between the misclassification rates of the modified and original OOB data, divided by the standard error, quantifies the variable's importance. This analysis helps identify the main factors influencing the model's predictions (Nyongesa, 2020). This method, known as permutation feature importance, directly estimate the influence of each predictor by observing how randomly reshuffling the variable affects the model's performance. The relative importance factors of the variables range from 0% to 100%, with the most crucial variable always having a relative importance of 100%. In order to compare these results to the Pearson's heatmap matrix, the latter values were considered only in modulus, since RF analysis outlines only positive values. It is important to point out that it is not recommended to normalize Pearson´s Heatmap matrix values once they already vary from 0 to 1 in modulus, and they were just adjusted to be presented as a percentage. As the linear coefficient is calculating between each variable (not considering others), the only way of having a value equal to one is when the variable's coefficient is calculated with itself.

Figure 10 illustrates the decreasing importance of variables in the sand-GM interface shear strength for the 14 influencing parameters evaluated by RF and Pearson's Matrix Heatmap. It can be seen that, except for the asperity height, normal stress and sand relative density, the values presented by the

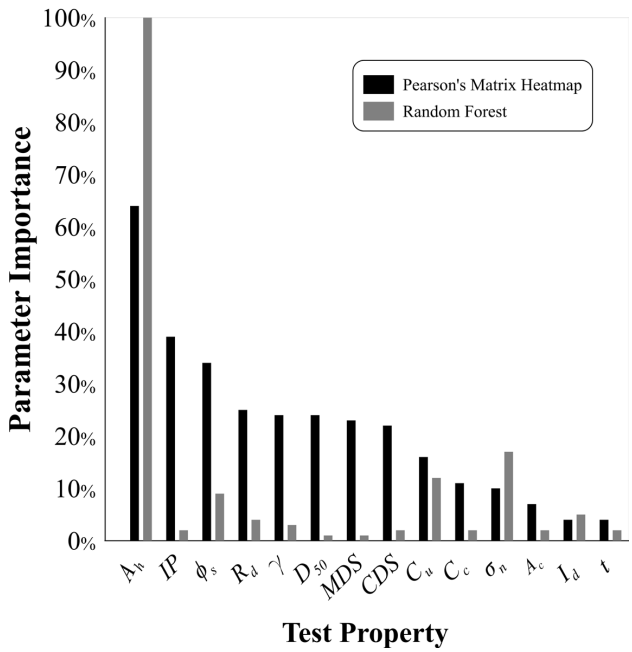


**Figure 10.** Importance of influential parameters.

Pearson matrix are much higher than the ones presented by the Random Forest analysis. This is attributed to the fact that the Pearson matrix is calculated based on a direct relation between the analysed property and the interface shear strength, which is different from the Random Forest method herein used. Similar to the $\rho_r$, the RF analysis revealed that the asperity height of the geomembrane exhibited the strongest impact on the interface shear strength, which is consistent with the results obtained in previous studies conducted by Stark et al. (1996), Lopes et al. (2001), Frost et al. (2012), Bacas et al. (2015), Cen et al. (2018), Araújo et al. (2022) and Costa Junior et al. (2023). In all these cases, there was an increment of the interface friction angle values for textured GM comparing with smooth GM due to the fact that the asperities block soil movement over the geomembrane.

According to the RF method, the applied normal stress was the second parameter ranked in terms of importance regarding the interface shear strength due to the need of higher shear stress to generate the interface failure (Negussey et al., 1989; Dove & Frost, 1999; Fleming et al., 2006; Sharma et al., 2007; Fox & Thielmann, 2014; Sánchez, 2018; Lashkari & Jamali, 2021; Afzali-Nejad et al., 2017; Chen et al., 2021; Khan & Latha, 2023). However, this was not observed in the Person's matrix, where the second most influential parameter was soil friction angle. The presented values showed that both factors influence on the results and the differences can also be attributed to how each method calculates this influence.

Overall, the results displayed that the soils properties such as soil friction angle ($\phi_s$), Soil median grain size ($D_{50}$), Uniformity Coefficient ($C_u$), Coefficient of Curvature ($C_c$), Relative density ($I_d$) and specific weight ($\gamma$) have an influence on the interface shear strength and this is in accordance with other investigations related to laboratory measurements (Costa e Lopes, 2001; Afonso, 2009; Choudhary & Krishna, 2016; Markou & Evangelou, 2018; Cen et al., 2018; Lashkari & Jamali, 2021; Ari & Akbulut, 2022; Khan & Latha, 2023). Among the soil properties ($\phi_s$, $\gamma$, $I_d$, $D_{50}$, $C_u$ and $C_c$), the Pearson's heatmap matrix indicated that $\phi_s$, $\gamma$ and $D_{50}$ have the highest influence on the interface strength while the Random Forest analysis outlined $C_u$, $\phi_s$, and $I_d$. Even though the observed differences, it can be noticed that the soil friction angle, soil relative density (related to the value of $\gamma$) and the grain size distribution have medium influence on the interface shear strength. The laboratory tests have shown this trend, but the analysis herein performed could quantify these effects comparing the different properties.

Regarding experiment settings, when observing the obtained values for the type of test, *IP* test has the higher influence for both methods herein utilized and the other two type of tests (*CDS* and *MDS*) presented slightly differences on the shear resistance depending on the used test. On the other hand, displacement rate ($R_d$) presented a high influence on the interface shear strength based on the Pearson´s matrix heat map and this influence was lower considering the RF analysis. This test configuration does influence the result over conducted laboratory tests as presented by the literature (Moraci et al., 2014; Carbone et al., 2015; Pavanello et al., 2021).

Both Machine Learning and linear regression methods outlined a very low influence of the geomembrane thickness ($t$) and contact area ($A_c$) on the interface resistance (Dove & Frost, 1999; Lima Junior, 2000; Wasti & Özdüzgün, 2001; Hsieh & Hsieh, 2003; Aguiar, 2008; Pitanga et al., 2009; Moraci et al., 2014; Sánchez, 2018). In order to assess if these properties influence on the interface, ML analysis were performed with and without them in the dataset. The results showed that despite the low linear correlation and higher data dispersion of these properties, including them in the analysis improved the model's ability to train the utilized data.

## 6. Conclusions

This study evaluated the use of two ML methodologies for predicting interface shear strength values between sand and GM. The dataset included 495 samples with 14 influencing parameters and interface friction angle results from laboratory tests. Four ANN models with varying inputs and hidden layers and a RF model following a nonlinear approach were implemented. Based on the relationship between predicted and actual values, the evaluation criteria utilized two statistical measures, $R^2$ and *RMSE*. The findings indicated the following conclusions:

- Overall, both Machine Learning methodologies (Random Forest and Artificial Neural Network) proved to be suitable for predicting interface friction angle results based on the collected data considering different types of experiments;

- Linear correlation (Pearson's coefficient) and the non-linear RF approach showed similar results for several influential factors on the interface shear strength, and the differences found are likely due to how each method does the calculation. The data analysis revealed that the GM asperity height had the most significant impact on interface shear strength. Soil properties and applied normal stress also found with considerable influence. The aforementioned is consistent with laboratory results obtained in different studies. The use of more data may improve the training and analysis of ML methodologies;
- The ANN model consisting of 14 inputs and two hidden layers exhibited the best predicted accuracy compared to the other three architectures for the analysed data. More hidden layers generated similar $R^2$ value but with more computational consuming time on the training and prediction process. Furthermore, the non-linear RF model demonstrated the highest accuracy in predicting interface strength values, slightly outperforming the ANN model.

## Acknowledgements

The authors would like to acknowledge the Conselho Nacional de Desenvolvimento Científico e Tecnológico - CNPq (Project number 404480/2021-7) and FAPDF (Project number 00193-00000846/2021-26) for the financial support provided for the development of this work. The authors also would like to thank the NORTENE Group for providing several test results that contributed to the research.

## Declaration of interest

The authors have no conflicts of interest to declare. All co-authors have observed and affirmed the contents of the paper and there is no financial interest to report.

## Authors' contributions

Anderson Villamil: conceptualization, data curation, visualization, writing – original draft. Abenezer Tefera Tanga: conceptualization, data curation, visualization, writing – original draft. Gregório Luís Silva Araújo: formal analysis, funding acquisition, investigation, methodology, project administration, resources. Francisco Evangelista Junior: supervision, validation, software writing – review & editing.

## Data availability

Data generated and analysed in the course of the current study are not publicly available due to copyrights.

## Declaration of use of generative artificial intelligence

This work was prepared with the assistance of generative artificial intelligence (GenAI) ChatGPT and Tyche software, with the aim of translation and for improving the quality of texts, data analysis and results, respectively. The entire process of using this tool was supervised, reviewed and when necessary edited by the authors. The authors assume full responsibility for the content of the publication that involved the aid of GenAI.

## List of symbols and abbreviations

| | |
|---|---|
| $n$ | Number of samples, data (dimensionless) |
| $t$ | Geomembrane thickness (mm) |
| $\overline{y}$ | Mean actual value |
| $y_i$ | Actual value |
| $\hat{y}_i$ | Expected or predicted value |
| $A_c$ | Contact area (cm$^2$) |
| $A_h$ | Geomembrane asperity height (mm) |
| AI | Artificial Intelligence |
| ANN | Artificial Neural Network |
| BP | Backpropagation |
| $C_c$ | Coefficient of curvature (dimensionless) |
| *CDS* | Conventional Direct Shear test |
| $C_u$ | Uniformity coefficient (dimensionless) |
| *CV* | Coefficient of Variation |
| DE | Differential Evolution |
| $D_{50}$ | Soil median grain size (mm) |
| EA | Evolutionary Algorithms |
| GM | Geomembrane(s) |
| HPO | Hyperparameter Optimisation |
| $I_d$ | Sand relative density (%) |
| *IP* | Inclined Plane test |
| *MDS* | Medium Direct Shear test |
| ML | Machine Learning |
| MLP | Multi-Layer Perceptron |
| OOB | Out-Of-Bag |
| $R_d$ | Displacement rate of the test (mm/min) |
| $R^2$ | Coefficient of Determination |
| $R^2$ | Coefficient of Determination |
| ReLU | Rectified Linear Unit function |
| RF | Random Forest |
| *RMSE* | Root Mean Squared Error |
| $\gamma$ | Soil unit weight (kN/m$^3$) |
| $\delta'$ | Friction angle interface (°) |
| $\rho_r$ | Pearson correlation coefficient |
| $\sigma_n$ | Normal stress (kPa) |
| $\sigma_{STD}$ | Standard deviation (dimensionless) |
| $\phi_s$ | Friction angle of soil (°) |

## References

Afonso, M.R.F.L. (2009). *Direct shear tests in the characterization of the soil-geosynthetic interface* [Master's dissertation]. University of Porto, Porto (in Portuguese).

Afzali-Nejad, A., Lashkari, A., & Shourijeh, P.T. (2017). Influence of particle shape on the shear strength and dilation of sand-woven geotextile interfaces. *Geotextiles and Geomembranes*, 45(1), 54-66. http://doi.org/10.1016/j.geotexmem.2016.07.005.

Aguiar, V.R. (2008). *Resistance of interfaces soil - geosynthetics - development of equipment and tests* [Doctoral thesis]. Pontifical Catholic University of Rio de Janeiro (in Portuguese).

Ali, T., Haider, W., Ali, N., & Aslam, M. (2022). A machine learning architecture replacing heavy instrumented laboratory tests: in application to the pullout capacity of geosynthetic reinforced soils. *Sensors*, 22(22), 8699. http://doi.org/10.3390/s22228699.

Alzahrani, S. (2017). *Effect of time on soil-geomembrane interface shear strength* [Master's dissertation]. University of Dayton, Dayton, OH. http://doi.org/10.13140/RG.2.2.25743.28320.

Araújo, G.L.S., Sánchez, N.P., Palmeira, E.M., & Almeida, M.G.G. (2022). Influence of micro and macroroughness of geomembrane surfaces on soil-geomembrane and geotextile-geomembrane interface strength. *Geotextiles and Geomembranes*, 50(4), 751-763. http://doi.org/10.1016/j.geotexmem.2022.03.015.

Ari, A., & Akbulut, S. (2022). Effect of fractal dimension on sand-geosynthetic interface shear strength. *Powder Technology*, 401, 117349. http://doi.org/10.1016/j.powtec.2022.117349.

Atangana Njock, P.G., Zhang, N., Zhou, A., & Shen, S.L. (2023). Evaluation of lateral displacement induced by jet grouting using improved Random Forest. *Geotechnical and Geological Engineering*, 41(1), 459-475. http://doi.org/10.1007/s10706-022-02270-y.

Bacas, B.M., Cañizal, J., & Konietzky, H. (2015). Shear strength behavior of geotextile/geomembrane interfaces. *Journal of Rock Mechanics and Geotechnical Engineering*, 7(6), 638-645. http://doi.org/10.1016/j.jrmge.2015.08.001.

Basheer, I.A., & Hajmeer, M. (2000). Artificial neural networks: Fundamentals, computing, design, and application. *Journal of Microbiological Methods*, 43(1), 3-31. http://doi.org/10.1016/S0167-7012(00)00201-3.

Borges, J.F., Paula, V.F., Evangelista Junior, F., & Bezerra, L.M. (2020). Reliability and uncertainty quantification of the net section tension capacity of cold-formed steel angles with bolted connections considering shear lag. *Advances in Structural Engineering*, 24(7), 1283-1296. http://doi.org/10.1177/1369433220971731.

Breiman, L. (2001). Random Forests. *Machine Learning*, 45(1), 5-32. http://doi.org/10.1023/A:1010933404324.

Carbone, L., Gourc, J.P., Carrubba, P., Pavanello, P., & Moraci, N. (2015). Dry friction behaviour of a geosynthetic interface using inclined plane and shaking table tests. *Geotextiles and Geomembranes*, 43(4), 293-306. http://doi.org/10.1016/j.geotexmem.2015.05.002.

Cen, W.-J., Wang, H., & Sun, Y.-J. (2018). Laboratory investigation of shear behavior of high-density polyethylene geomembrane interfaces. *Polymers*, 10(7), 734. http://doi.org/10.3390/polym10070734.

Chao, Z., Fowmes, G., & Dassanayake, S.M. (2021). Comparative study of hybrid artificial intelligence approaches for predicting peak shear strength along soil-geocomposite drainage layer interfaces. *International Journal of Geosynthetics and Ground Engineering*, 7(3), 60. http://doi.org/10.1007/s40891-021-00299-2.

Chao, Z., Shi, D., Fowmes, G., Xu, X., Yue, W., Cui, P., Hu, T., & Yang, C. (2023). Artificial intelligence algorithms for predicting peak shear strength of clayey soil-geomembrane interfaces and experimental validation. *Geotextiles and Geomembranes*, 51(1), 179-198. http://doi.org/10.1016/j.geotexmem.2022.10.007.

Chaves, J.F.N., Evangelista Junior, F., Rego, J.H.S., & Vasques, L.P. (2023). Dataset construction and data science analysis of physicochemical characterization of ordinary Portland cement. *Revista IBRACON de Estruturas e Materiais*, 16(6), e16609. http://doi.org/10.1590/s1983-41952023000600009.

Chen, W.-B., Xu, T., & Zhou, W.-H. (2021). Microanalysis of smooth Geomembrane–Sand interface using FDM–DEM coupling simulation. *Geotextiles and Geomembranes*, 49(1), 276-288. http://doi.org/10.1016/j.geotexmem.2020.10.022.

Choudhary, A., & Krishna, A.M. (2016). Experimental investigation of interface behaviour of different types of granular soil/geosynthetics. *International Journal of Geosynthetics and Ground Engineering*, 1(2), 4. http://doi.org/10.1007/s40891-016-0044-8.

Costa e Lopes, C.P.F. (2001). *Study of soil-geosynthetic interaction through inclined plane shear tests* [Master's dissertation]. University of Porto, Porto (in Portuguese).

Costa Junior, S.L., Aparicio-Ardila, M.A., Palomino, C.F., & Lins da Silva, J. (2023). Analysis of textured geomembrane-soil interface strength to mining applications. *International Journal of Geosynthetics and Ground Engineering*, 9(1), 3. http://doi.org/10.1007/s40891-022-00423-w.

Debnath, P., & Dey, A.K. (2017). Prediction of laboratory peak shear stress along the cohesive soil-geosynthetic interface using artificial neural network. *Geotechnical and Geological Engineering*, 35(1), 445-461. http://doi.org/10.1007/s10706-016-0119-2.

Dede, T., Kankal, M., Vosoughi, A.R., Grzywiński, M., & Kripka, M. (2019). Artificial Intelligence applications in civil engineering. *Advances in Civil Engineering*, 1-3(1), 8384523. http://doi.org/10.1155/2019/8384523.

Diaz, G.I., Fokoue-Nkoutche, A., Nannicini, G., & Samulowitz, H. (2017). An effective algorithm for hyperparameter optimization of neural networks. *IBM Journal of Research and Development*, 61, 9:1-9:11. http://doi.org/10.1147/JRD.2017.2709578.

Dove, J.E., & Frost, J.D. (1999). Peak friction behavior of smooth geomembrane-particle interfaces. *Journal of Geotechnical and Geoenvironmental Engineering*, 125(7), 544-555. http://doi.org/10.1061/(ASCE)1090-0241(1999)125:7(544).

Evangelista Junior, F., & Afanador-García, N. (2016). A polynomial chaos expansion approach to the analysis of uncertainty in viscoelastic structural elements. *Dyna*, 83(199), 172-182. http://doi.org/10.15446/dyna.v83n199.53834.

Evangelista Junior, F., & Almeida, I.F. (2021). Machine learning RBF-based surrogate models for uncertainty quantification of age and time-dependent fracture mechanics. *Engineering Fracture Mechanics*, 258, e108037. http://doi.org/10.1016/j.engfracmech.2021.108037.

Fausett, L. (1994). *Fundamentals of neural networks: architectures, algorithms and applications* (1st ed.). Englewood Cliffs: Prentice Hall.

Fleming, I.R., Sharma, J.S., & Jogi, M.B. (2006). Shear strength of geomembrane-soil interface under unsaturated conditions. *Geotextiles and Geomembranes*, 24(5), 274-284. http://doi.org/10.1016/j.geotexmem.2006.03.009.

Fox, P.J., & Thielmann, S.S. (2014). Interface Shear Damage to a HDPE Geomembrane. II: Gravel Drainage Layer. *Journal of Geotechnical and Geoenvironmental Engineering*, 140(8), 04014040. http://doi.org/10.1061/(ASCE)GT.1943-5606.0001120.

Frost, J., Kim, D., & Lee, S. (2012). Microscale geomembrane-granular material interactions. *KSCE Journal of Civil Engineering*, 16(1), 79-92. http://doi.org/10.1007/s12205-012-1476-x.

Géron, A. (2019). *Hands-on machine learning with Scikit-Learn, Keras and TensorFlow: concepts, tools, and techniques to build intelligent systems* (2nd ed.). Beijing: O'Really Media, Inc.

Glorot, X., Bordes, A., & Bengio, Y. (2011). Deep sparse rectifier neural networks. In *Proceedings of the 14th International Conference on Artificial Intelligence and Statistics* (Vol. 15, pp. 315-323), Fort Lauderdale, FL. Retrieved in March 12, 2025, from https://proceedings.mlr.press/v15/glorot11a/glorot11a.pdf

Gourc, J.P., & Reyes Ramírez, R. (2004). Dynamics-based interpretation of the interface friction test at the inclined plane. *Geosynthetics International*, 11(6), 439-454. http://doi.org/10.1680/gein.2004.11.6.439.

Hasthi, V., Nouman Amjad, M., Hegde, A., & Shukla, S.K. (2022). Experimental and intelligent modelling for predicting the amplitude of footing resting on geocell-reinforced soil bed under vibratory load. *Transportation Geotechnics*, 35, 100783. http://doi.org/10.1016/j.trgeo.2022.100783.

Hsieh, C., & Hsieh, M.-W. (2003). Load plate rigidity and scale effects on the frictional behavior of sand/geomembrane interfaces. *Geotextiles and Geomembranes*, 21(1), 25-47. http://doi.org/10.1016/S0266-1144(02)00034-1.

Hsieh, C., Hsieh, M.-W., & Chein, J. (2002). Direct shear behaviour of sand geomembrane systems of various shear boxes. In *Proceedings of the 7th ICG - Geotechnical Engineering and Reinforced Structures* (Vol. 2, pp. 671-676), Nice, France.

Huang, Y., Li, J., & Fu, J. (2019). Review on application of artificial intelligence in civil engineering. *Computer Modeling in Engineering & Sciences*, 121(3), 845-875. http://doi.org/10.32604/cmes.2019.07653.

Hutter, F., Kotthoff, L., & Vanschoren, J. (2019). *Automated machine learning: methods, systems, challenges*. Cham: Springer.

Industry Data. (2021). *Report of direct shear tests.* São Paulo.

Izgin, M. (1997). *Geomembrane-sand interface friction* [Master's dissertation]. Middle East Technical University, Turkey.

Izgin, M., & Wasti, Y. (1998). Geomembrane-sand interface frictional properties as determined by inclined board and shear box tests. *Geotextiles and Geomembranes*, 16(4), 207-219. http://doi.org/10.1016/S0266-1144(98)00010-7.

Jeremiah, J.J., Abbey, S.J., Booth, C.A., & Kashyap, A. (2021). Results of application of artificial neural networks in predicting geo-mechanical properties of stabilised clays: a review. *Geotechnics*, 1(1), 147-171. http://doi.org/10.3390/geotechnics1010008.

Khan, R., & Latha, G.M. (2023). Multi-scale understanding of sand-geosynthetic interface shear response through Micro-CT and shear band analysis. *Geotextiles and Geomembranes*, 51(3), 437-453. http://doi.org/10.1016/j.geotexmem.2023.01.006.

Koerner, R.M. (2012). *Designing with geosynthetics.* Englewood Cliffs: Prentice Hall.

Koutsourais, M.M., & Sprague, C. J. (1991). Interfacial friction study of cap and liner components for landfill design. *Geotextiles and Geomembranes*, 10(5-6), 531-548. http://doi.org/10.1016/0266-1144(91)90045-X.

Kumari, S., & Dutta, R.K. (2019). Leakage rate prediction through composite liner due to geomembrane defect using neural network. *Journal of Geotechnical Engineering*, 6(3), 8-17.

Lagaros, N.D., & Plevris, V. (2022). Artificial Intelligence (AI) applied in civil engineering. *Applied Sciences*, 12(15), 7595. http://doi.org/10.3390/app12157595.

Lashkari, A., & Jamali, V. (2021). Global and local sand–geosynthetic interface behaviour. *Geotechnique*, 71(4), 346-367. http://doi.org/10.1680/jgeot.19.P.109.

Li, D., Jiang, Z., Tian, K., & Ji, R. (2025). Prediction of hydraulic conductivity of sodium bentonite GCLs by machine learning approaches. *Environmental Geotechnics*, 12(2), 154-173. http://doi.org/10.1680/jenge.22.00181.

Liaw, A., & Wiener, M. (2002). Classification and regression by Random Forest. *The R Journal*, 2/3, 18-22. Retrieved in March 12, 2025, from https://journal.r-project.org/issues/2002-3/2002-3.pdf

Lima Junior, N.R. (2000). *Study of the soil-geosynthetic interaction in environmental protection works using the inclined plane equipment* [Master's dissertation]. University of Brasilia, Brasília (in Portuguese).

Lima, J.P.S., Evangelista Junior, F., & Soares, C.G. (2023a). Bi-fidelity Kriging model for reliability analysis of the ultimate strength of stiffened panels. *Marine Structures*, 91, 103464. http://doi.org/10.1016/j.marstruc.2023.103464.

Lima, J.P.S., Evangelista Junior, F., & Soares, C.G. (2023b). Hyperparameter-optimized multi-fidelity deep neural network model associated with subset simulation for structural reliability analysis. *Reliability Engineering & System Safety*, 1, 109492. http://doi.org/10.1016/j.ress.2023.109492.

Lopes, P.C., Lopes, M.L., & Lopes, M.P. (2001). Shear behaviour of geosynthetics in the inclined plane test: influence of soil particle size and geosynthetic structure. *Geosynthetics International*, 8(4), 327-342. http://doi.org/10.1680/gein.8.0198.

Lu, P., Chen, S., & Zheng, Y. (2012). Artificial Intelligence in Civil Engineering. *Mathematical Problems in Engineering*, 2012(1), 1-22. http://doi.org/10.1155/2012/145974.

Markou, I.N., & Evangelou, E.D. (2018). Shear Resistance Characteristics of Soil–Geomembrane Interfaces. *International Journal of Geosynthetics and Ground Engineering*, 4(4), 29. http://doi.org/10.1007/s40891-018-0146-6.

Mello, L.G.R. (2001). *Study of the soil-geosynthetic interaction in slopes of waste disposal works* [Master's dissertation]. University of Brasilia, Brasília (in Portuguese).

Moraci, N., Cardile, G., Gioffrè, D., Mandaglio, M.C., Calvarano, L.S., & Carbone, L. (2014). Soil geosynthetic interaction: design parameters from experimental and theoretical analysis. *Transportation Infrastructure Geotechnology*, 1(2), 165-227. http://doi.org/10.1007/s40515-014-0007-2.

Negussey, D., Wijewickreme, W.K.D., & Vaid, Y.P. (1989). Geomembrane interface friction. *Canadian Geotechnical Journal*, 26(1), 165-169. http://doi.org/10.1139/t89-018.

Nyongesa, D. (2020). Variable selection using Random Forests in SAS. In *Proceedings of the SAS Global Forum.* Retrieved in March 12, 2025, from https://support.sas.com/resources/papers/proceedings20/4826-2020.pdf

O'Rourke, T.D., Druschel, S.J., & Netravali, A.N. (1990). Shear strength characteristics of sand-polymer interfaces. *Journal of Geotechnical Engineering*, 116(3), 451-469. http://doi.org/10.1061/(ASCE)0733-9410(1990)116:3(451).

Oliveira, T.A.A., Gomes, G., & Evangelista Junior, F. (2019). Multiscale aircraft fuselage fatigue analysis by the dual boundary element method. *Engineering Analysis with Boundary Elements*, 104, 107-119. http://doi.org/10.1016/j.enganabound.2019.03.032.

Palmeira, E.M. (2009). Soil-geosynthetic interaction: modelling and analysis. *Geotextiles and Geomembranes*, 27(5), 368-390. http://doi.org/10.1016/j.geotexmem.2009.03.003.

Palmeira, E.M., Lima Junior, N.R., & Mello, L.G.R. (2002). Interaction between soils and geosynthetic layers in large-scale ramp tests. *Geosynthetics International*, 9(2), 149-187. http://doi.org/10.1680/gein.9.0214.

Pant, A., & Ramana, G.V. (2022). Novel application of machine learning for estimation of pullout coefficient of geogrid. *Geosynthetics International*, 29(4), 342-355. http://doi.org/10.1680/jgein.21.00021a.

Pavanello, P., Carrubba, P., & Moraci, N. (2021). The characterisation of geosynthetic interface friction by means of the inclined plane test. *Geotextiles and Geomembranes*, 49(1), 257-275. http://doi.org/10.1016/j.geotexmem.2020.10.027.

Pitanga, H.N., Gourc, J.-P., & Vilar, O.M. (2009). Interface shear strength of geosynthetics: evaluation and analysis of inclined plane tests. *Geotextiles and Geomembranes*, 27(6), 435-446. http://doi.org/10.1016/j.geotexmem.2009.05.003.

Raja, M.N.A., & Shukla, S.K. (2021). Predicting the settlement of geosynthetic-reinforced soil foundations using evolutionary artificial intelligence technique. *Geotextiles and Geomembranes*, 49(5), 1280-1293. http://doi.org/10.1016/j.geotexmem.2021.04.007.

Raja, M.N.A., Shukla, S.K., & Khan, M.U.A. (2022). An intelligent approach for predicting the strength of geosynthetic-reinforced subgrade soil. *International Journal of Pavement Engineering*, 23(10), 3505-3521. http://doi.org/10.1080/10298436.2021.1904237.

Rebelo, K.M.W. (2003). *Interface strength between geomembranes and soils by ring shear test* [Master's dissertation]. University of São Paulo, São Carlos. http://doi.org/10.11606/D.18.2003.tde-10052004-164052.

Reyes Ramirez, R., & Gourc, J.P. (2003). Use of the inclined plane test in measuring geosynthetic interface friction relationship. *Geosynthetics International*, 10(5), 165-175. http://doi.org/10.1680/gein.2003.10.5.165.

Sánchez, N.P. (2018). *Study of some aspects that influence the adhesion between geosynthetics and different materials* [Doctoral thesis]. University of Brasilia, Brasília (in Portuguese).

Schober, P., Boer, C., & Schwarte, L.A. (2018). Correlation coefficients: appropriate use and interpretation. *Anesthesia and Analgesia*, 126(5), 1763-1768. http://doi.org/10.1213/ANE.0000000000002864.

Shahin, M.A. (2013). Artificial intelligence in geotechnical engineering. In X.S. Yang, A.H. Gandomi, S. Talatahari & A.H. Alavi (Eds.), *Metaheuristics in water, geotechnical and transport engineering* (pp. 169-204). Cham: Elsevier. http://doi.org/10.1016/B978-0-12-398296-4.00008-8.

Shahin, M.A., Jaksa, M.B., & Maier, H.R. (2008). State of the art of artificial neural networks in geotechnical engineering. *The Electronic Journal of Geotechnical Engineering*, 8, 1-26.

Shahin, M.A., Jaksa, M.B., & Maier, H.R. (2009). Recent advances and future challenges for artificial neural systems in geotechnical engineering applications. *Advances in Artificial Neural Systems*, 308239(1), 1-9. http://doi.org/10.1155/2009/308239.

Sharma, J.S., Fleming, I.R., & Jogi, M.B. (2007). Measurement of unsaturated soil: geomembrane interface shear-strength parameters. *Canadian Geotechnical Journal*, 44(1), 78-88. http://doi.org/10.1139/t06-097.

Silva, V.P., Carvalho, R.D.A., Rêgo, J.H.D.S., & Evangelista Junior, F. (2023). Machine learning-based prediction of the compressive strength of Brazilian concretes: a dual-dataset study. *Materials*, 16(14), 4977. http://doi.org/10.3390/ma16144977.

Soleimanbeigi, A., & Hataf, N. (2006). Prediction of settlement of shallow foundations on reinforced soils using neural networks. *Geosynthetics International*, 13(4), 161-170. http://doi.org/10.1680/gein.2006.13.4.161.

Stark, T.D., Williamson, T.A., & Eid, H.T. (1996). HDPE geomembrane/geotextile interface shear strength. *Journal of Geotechnical Engineering*, 122(3), 197-203. http://doi.org/10.1061/(ASCE)0733-9410(1996)122:3(197).

Storn, R., & Price, K. (1996). Minimizing the real functions of the ICEC'96 contest by differential evolution. In *Proceedings of IEEE International Conference on Evolutionary Computation* (pp. 842-844), Nagoya, Japan. New York: IEEE. http://doi.org/10.1109/ICEC.1996.542711.

Tan, Y., Chen, J., & Benson, C. H. (2022). Predicting hydraulic conductivity of geosynthetic clay liners using a neural network algorithm. In *Proceedings of the Geo-Congress 2022* (pp. 21-28), Charlotte, North Carolina. http://doi.org/10.1061/9780784484050.003.

Tyche. (2023). *Data science and artificial intelligence software. Machine learning module, version 2.0.* Brasília: Computational Methods and Artificial Intelligence Laboratory (LAMCIA), Nexum Research Group, Universidade de Brasília.

Vangla, P., & Gali, M.L. (2016). Shear behavior of sand - smooth geomembrane interfaces through micro - topographical analysis. *Geotextiles and Geomembranes*, 44(4), 592-603. http://doi.org/10.1016/j.geotexmem.2016.04.001.

Viana, H.N.L. (2007). *Study on the soil–geosynthetic interaction in slopes of waste disposal facilities* [Doctoral thesis]. University of Brasilia, Brasília (in Portuguese).

Wasti, Y., & Özdüzgün, Z.B. (2001). Geomembrane–geotextile interface shear properties as determined by inclined board and direct shear box tests. *Geotextiles and Geomembranes*, 19(1), 45-57. http://doi.org/10.1016/S0266-1144(00)00002-9.

Xu, M., Zhou, Y., Pang, R., & Xu, B. (2023). Seismic collaborative reliability evaluation of slopes using subset simulation via support vector machine. *Soil Dynamics and Earthquake Engineering*, 165, 107673. http://doi.org/10.1016/j.soildyn.2022.107673.

Yu, T., & Zhu, H. (2020). Hyper-parameter optimization: a review of algorithms and applications. *Computer Science*, http://doi.org/10.48550/arXiv.2003.05689.